PNAS
www.pnas.org

Supplementary Information for

Aldehyde Dehydrogenase 3A1 Activation Prevents Radiation-Induced Xerostomia by Protecting Salivary Stem Cells from Toxic Aldehydes

Julie P. Saiki, Hongbin Cao, Lauren D. Van Wassenhove, Vignesh Viswanathan, Joshua Bloomstein, Dhanya K. Nambiar, Aaron J. Mattingly, Dadi Jiang, Che-Hong Chen, Matthew C. Stevens, Amanda L. Simmons, Hyun Shin Park, Rie von Eyben, Eric T. Kool, Davud Sirjani, Sarah M. Knox, Quynh Thu Le, Daria Mochly-Rosen

Daria Mochly-Rosen
mochly@stanford.edu

Quynh Thu Le
qle@stanford.edu

This PDF file includes:

Supplementary text
Figs. S1 to S7
Table S1
References for SI reference citations

www.pnas.org/cgi/doi/10.1073/pnas.1802184115

Supplementary Information Text

Supplemental Methods

Drugs. A library of TCM plants was donated to the DM-R laboratory by Sun Ten Pharmaceutical Co. in Taiwan. D-limonene, all other screened compounds, and pilocarpine were purchased from Sigma-Aldrich. Isoflurane (VetOne), ketamine (VEDCO), and xylazine (AnaSEd) were acquired through Stanford University's Veterinary Service Center.

Salisphere formation assay. Mouse salivary gland cells were isolated as previously described (1). Mouse submandibular glands (SMG) were homogenized and incubated in DMEM/F12 with collagenase (0.025%) and hyaluronidase (0.04%) (Stem Cell Technologies), 6.25 mM CaCl, and an antifungal (Omega Scientific; 1:500) for 1 h and in dispase (BD Biosciences) for 1 h on a shaker at 37°C. Tissue was filtered through a 100 μM cell strainer and centrifuged at 1200 rpm for 6 min. Red blood cells were lysed with ACK Lysing Buffer (Lonza) for 2 min, inactivated with 10% FBS DMEM, filtered through 100 μM cell strainer, and centrifuged at 1200 rpm for 6 min. Cells were then trypsinized with 0.25% trypsin for 1 min, inactivated with 10% FBS DMEM, filtered through a 40 μM cell strainer, and centrifuged at 1200 rpm for 6 min. Dissociated cells were seeded on matrigel (BD Biosciences) and grown in DMEM/F12+GlutaMax (Gibco) media containing 10% FBS, 1x antibiotic-antimycotic (Gibco), 1% N2 supplement (Gibco), 20 ng/mL epidermal growth factor-2 (Sigma-Aldrich), 20 ng/mL fibroblast growth factor-2 (Sigma-Aldrich), 10 μg/mL insulin (Sigma-Aldrich), 1 μM dexamethasone (Sigma-Aldrich), 10 μM Y-27632 (Stem Cell Technologies). Spheres were grown for 7 d, imaged using a Leica DMi8 microscope at 2.5x magnification, and quantified with ImageJ (NIH).

DarkZone dye aldehyde assay in murine salispheres. Cells isolated from mouse SMG were grown into spheres in DMEM/F12+GlutaMax (Gibco) media containing 10% FBS, 1x antibiotic-antimycotic (Gibco), 1% N2 supplement (Gibco), 20 ng/mL epidermal growth factor-2 (Sigma-Aldrich), 20 ng/mL fibroblast growth factor-2 (Sigma-Aldrich), 10 μg/mL insulin (Sigma-Aldrich), 1 μM dexamethasone (Sigma-Aldrich), 10 μM Y-27632 (Stem Cell Technologies). Spheres were dissociated in sterile PBS with 2% FBS, irradiated with 4 Gy, and incubated at 37°C for 2 h. Cells were then stained with 20 uM DarkZone fluorescein aldehyde dye synthesized by the laboratory of Dr. Eric Kool at Stanford University (Stanford, CA) (3) and 10 mM 2,4-Dimethoxyaniline catalyst (TCI America) for 15 min at 37°C. Cells were washed twice with PBS and analyzed by flow cytometry. Data were represented as the average median fluorescence intensity.

DarkZone dye aldehyde assay in intact E13.5 embryonic SMG. E13.5 embryonic whole SMG were manually dissected from pregnant CD-1/ICR or C57BL6/J mice and cultured in DMEM/F12 with 50 ug/mL transferrin and 50 μg/mL Vitamin C for 24 h (4). Glands were irradiated with 4 or 8 Gy and incubated with 20 uM DarkZone fluorescein aldehyde dye (Stanford, CA) and 10 mM 2,4-Dimethoxyaniline catalyst (TCI America) for 1 h (3). Glands were imaged 3 h after IR using a Keyence BZ-X710 microscope GFP filter at 10x magnification. Average fluorescence intensity was quantified using ImageJ (NIH).

ALDH enzymatic assay. Isozymes of ALDH1A1, ALDH1A2, ALDH2, ALDH3A1, ALDH3A2, ALDH4A1, ALDH5A1, ALDH7A1 were measured as previously described using 5 μg/ml of recombinant protein (2). Briefly, enzymatic activity was measured spectrophotometrically by the reduction of NAD^+ to NADH at A_{340} over 5 min in the presence of increasing concentrations of D-limonene or DMSO vehicle control. Assays were conducted in 50 mM sodium pyrophosphate

buffer (pH 7.4) in the presence of 2.5 mM NAD^+ and 10 mM substrate and measured at 25°C. Dose-response curve fits and EC_{50}'s were calculated using GraphPad Prism 7 software.

ALDH fluorescence-coupled enzymatic assay. ALDH enzyme activity was measured in cell lysate or using recombinant ALDH1A1, ALDH1A2, ALDH3A1 by the reduction of NAD^+ to NADH amplified by the diaphorase conversation of resazurin to fluorescent resorufin (excitation 565 nm and emission 590 nm) as previously described (5) over 5 min in the presence of D-limonene or DMSO vehicle control. Assay conditions were modified from the original enzyme assay protocol above using 50 mM sodium pyrophosphate buffer (pH 7.4), 2.5 mM NAD^+, 10 mM acetaldehyde or all-trans-retinal as substrates with the addition of 1 U/mL diaphorase and 0.1 mM resazurin for the secondary reaction. Measurements were collected at 25°C.

Docking of D-limonene. Crystal structure files were downloaded from the RCSB PDB: ALDH2 (3INJ) and ALDH3A1 (3SZA). Each crystal structure was prepared for docking using Schrödinger suite Protein Preparation Wizard (6). The structures were preprocessed to fill in missing hydrogens and side chains, extra subunits were removed to leave a single ALDH monomer, and structures were automatically minimized with an OPLS3 force field. The receptor for each of the prepared protein structures was generated using the Schrödinger Receptor Grid Generation function (7) with default parameters. For ALDH2 (3INJ), the grid was generated around the co-crystallized Alda-1 ligand. For ALDH3A1 (3SZA), the grid was centered around the site (analogous to the ALDH2 Alda-1 binding site) identified through the SiteMap (8) function. D-limonene was prepared for docking using LigPrep. D-limonene was docked (9) to both ALDH2 and ALDH3A1 using their respective generated grids. Default settings for the Ligand Docking program were used, and no additional constraints were applied. We allowed for at most 40 poses per ligand to be written following post-docking minimization and selected the highest ranked pose for each enzyme for final analysis.

Stimulated saliva collection. 9-11 wk old female C57BL/6J WT mice or C57BL6 *Aldh3a1*$^{-/-}$ (from the laboratory of Dr. Vasilis Vasiliou at Yale University) were treated with 10% D-limonene mixed in chow or no treatment. 15 Gy single dose or 30 Gy fractionated over 5 d (6 Gy/d) were delivered to the SMG with the rest of the body lead shielded. Stimulated saliva was measured as previously described (10). Mice were anesthetized with a ketamine (80 mg/kg) and xylazine (16 mg/kg) mixture delivered by intraperitoneal injection and subcutaneously injected with 2 mg/kg pilocarpine. Saliva was collected for 15 min. Saliva volume was calculated by assuming that the density equals 1 mg/μL and was normalized to the mouse body weight by dividing the total collected saliva volume by the mouse weight (kg).

Periodic acid-Schiff staining and acinar quantification. SMG were removed from mice, fixed in 10% formalin for 24 h, and paraffin-embedded. Sections were deparaffinized, rehydrated, and stained with Periodic acid-Schiff staining (0.5% Periodic acid). 10 images per group were collected at random at 30x magnification using a Leica DM6000 B microscope. Acinar regions were quantified using RT_Image software (11). Images were separated into red, green, and blue color channels, blurred using a 20-pixel box filter, and segmented using an intensity contour of 110 with a minimum area of 100 um^2. Acinar area was calculated as a percentage of acinar area relative to the area of the microscopy field.

RNA-sequencing. Samples were extracted using Qiagen miRNeasy Kit (217084). Extracted samples were assessed for quality using Agilent Pico-RNA bio-analyzer chip (5067-1513). The Smarter Ultra Low Input RNA kit (Clontech, 634848) was used to generate cDNA from total RNA. Amplified cDNA was purified using SPRI Ampure Beads from Beckman Coulter, and quality and quantity were measured using a High Sensitivity DNA chip on an Agilent 2100 Bioanalyzer. cDNA was sheared to an average length of 300BP using a Covaris S2, and libraries were generated following the Clontech Low Input Library Prep kit (634947). Indexed libraries

were pooled and quantitated for sequencing. Sequencing data were generated on an Illumina HiSeq 4000 at the Stanford Functional Genomics Facility. The processed RNA-seq reads were imported into BRB-ArrayTools, an integrated package for the visualization and statistical analysis of gene expression data developed by Dr. Richard Simon and BRB-ArrayTools Development Team (Biometric Research Program, National Cancer Institute). The imported expression values were log2-transformed and subjected to quantile normalization by Robust Multi-chip Average (RMA). Genes that showed differential expression between control and irradiated groups (univariate p-value < 0.01) were selected. To identify functional networks and pathways enriched in these significant genes, we analyzed these genes using MetaCore (GeneGo). To generate the heatmaps, we used the clustering function of ArrayTools with experimental samples in fixed grouping and order. Genes were ordered by hierarchical clustering. Color scales of the individual heatmaps are shown. From these heatmaps, genes that share similar differential expression patterns were identified.

Annexin V/propidium iodide apoptosis assay. $EpCAM^+$-sorted salivary sphere cells were grown in matrigel as described above and treated with vehicle control (PEG-400) or 100 μM D-limonene for 48 h. Cells were dissociated from matrigel, stained with FITC Annexin V Apoptosis Detection Kit (Biolegend) and with Propidium Iodide (Life Technologies), and analyzed by flow cytometry. Annexin V^+PI^- cells were analyzed as early apoptotic cells, and Annexin V^+PI^+ cells were analyzed as late apoptotic cells.

Cleaved caspase-3 staining. SMG were removed from mice, fixed in 10% formalin for 24 h, and paraffin-embedded. Sections were stained with Caspase 3 rabbit antibody (1:200, Cell Signaling) and DAPI. Three random images using red and blue filters were taken at 100x magnification with a Leica DM6000 B microscope from each gland and quantified by counting cleaved caspase-3 positive (red) cells per field.

Phase 0 study in head and neck cancer patients. This study was approved by Stanford University's Institutional Review Board. Patients diagnosed with salivary gland tumors and scheduled to undergo salivary gland surgery were recruited for this 2-wk, open-label, oral disposition study of D-limonene. Patients were required to be between 18 to 85 years of age, have elected to undergo surgery for recent diagnosis of parotid or submandibular gland tumor, and qualified for anesthesia. Written informed consent was obtained from all patients before any study procedure was conducted. Patients were excluded from study participation if nursing or pregnant or diagnosed with kidney disease, end-stage liver disease, metastatic cancer, or any unstable medical condition. Four subjects began D-limonene treatment at 2 g/d (1 g twice daily) for 14 d during the period immediately before surgery. Blood and saliva samples were collected at baseline and on the day of surgery. Normal and tumor salivary gland tissues were collected during surgery. Drug levels in tissue, plasma, and saliva were measured by the GC-MS method described below.

Gas chromatography mass spectrometry. Human salivary gland samples were prepared using 25% tissue homogenate in phosphate buffer, spiked with 10,000 ng/mL perillyl aldehyde (in acetonitrile) as an internal standard, and extracted with heptane. An aliquot of the heptane layer was used for analysis. D-limonene concentrations were measured using an Agilent 7890/5975C GC/MSD equipped with an Agilent 7693 autosampler. Sample volumes of 1 μL splitless were injected with an inlet temperature of 220°C. The flow rate was constant at 1 mL/min. An Agilent DB-5MS UI column was used (30 m length, 0.250 mm inner diameter, 0.25 μm film). The temperature was held at 60°C for 1 min, increased to 150°C at a rate of 30°C/min, increased to 320°C at 60°C/min, and held for 3.167 min for a total run time of 10 min. Calibration curves were

linear from 4 to 8000 ng/mL. Experiments were conducted at the Stanford Mass Spectrometry Facility.

Methanol and hexane extractions of traditional Chinese medicine plants. 10 g of raw material were soaked in 100 mL of methanol or hexane overnight at 37°C on a shaker. The mixture was passed through qualitative filter paper (GE Healthcare Life Sciences Whatman, 270 mm diameter, grade 1). The remaining unfiltered material was soaked in 100 mL of methanol or hexane for an additional 2 h. The second mixture was passed through a qualitative filter paper. The two filtrates were combined for a total volume of 200 mL and concentrated to 20 mL using a rotavapor (Buchi R-100). 1 mL was further concentrated to a powder using a vacuum.

High Performance Liquid Chromatography. Active TCM extracts were fractionated with a 1:2 mixture of water and acetonitrile and fractionated by reversed-phase HPLC (Agilent 1260 Infinity, C18 column, 250 x 4.6 mm). A linear gradient of water to acetonitrile (5% to 100%) over 30 min at a flow rate of 0.65 ml/min was used. Fractions were collected once per min using an autosample collector.

Nuclear Magnetic Resonance. 1D 1H NMR spectra were acquired at the Stanford Magnetic Resonance Laboratory on a Bruker Avance 500 MHz spectrometer (TopSpin v1.3) with sample temperature regulated to 25˚C, 30˚ pulse, 16-264 scans, 1 sec pre-scan delay, 65536 total data points, 10330.58 Hz spectral width. Data were processed and analyzed using ACD Labs SpecHPLCtrus Processor.

Xenograft study. Six-wk old SCID mice (Jackson Labs) were implanted with SAS or SCC90 cells (2 x 10^6 cells/injection) into both flanks of each mouse. D-limonene was delivered orally (10% in chow) starting 1 wk before IR and continuing daily during and after IR. 30 Gy over 5 fractions (6 Gy/d) was delivered to the tumor site with the rest of the body shielded. Tumor size was measured every 1-2 d. Tumor volume was calculated using the formula (π x length x width x height)/6.

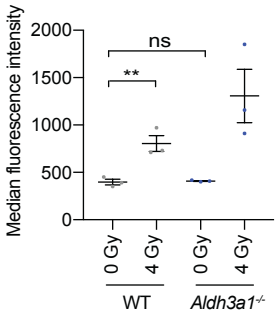

Fig. S1. Aldehyde levels in salispheres measured by DarkZone dye

Aldehyde levels in dissociated primary WT and *Aldh3a1*$^{-/-}$ salisphere cells were measured by DarkZone dye fluorescence intensity. This experiment was repeated in Fig. 1A but the data here show that there is a statistically significant increase in aldehyde levels in irradiated WT cells compared with nonirradiated WT cells. Aldehyde levels in nonirradiated WT and nonirradiated *Aldh3a1*$^{-/-}$ cells were not significantly different. (n=3; bars represent SEM; **=$p<0.01$).

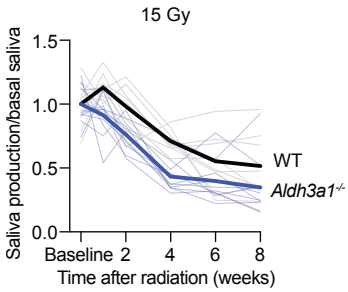

Fig. S2. Saliva production levels in WT and *Aldh3a1*$^{-/-}$ mice after 15 Gy

Individual mouse data of pilocarpine-induced saliva production collected in female C57BL/6J WT and *Aldh3a1*$^{-/-}$ mice at baseline and 1, 2, 4, 6, and 8 wk after 15 Gy (single dose). (n=8-11; thick lines represent mean; thin lines represent individual mice; wk 1 p=0.0071; wk 2 p=0.0067; wk 4 p=0.0008; wk 6 p=0.0531; wk 8 p=0.0374).

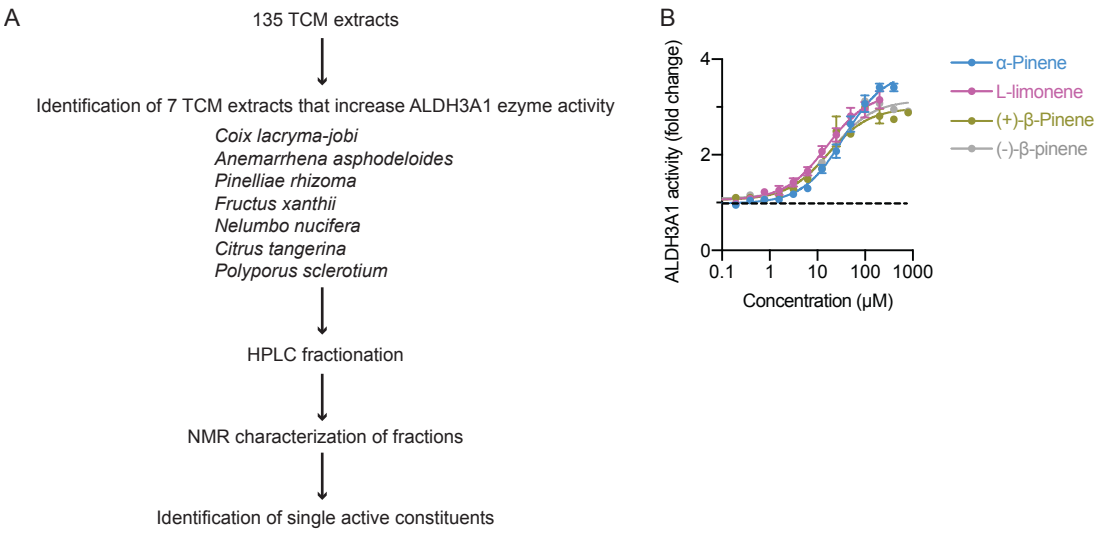

Fig. S3. TCM library screen and single active constituent identification by HPLC and NMR

(A) Workflow representing TCM library screen by spectrophotometric ALDH enzyme activity assay and the identification of 7 TCM extracts that increased ALDH3A1 catalytic activity. Active extracts were fractionated by HPLC, and active fractions were characterized by NMR in order to identify single active constituents. *(B)* ALDH3A1 activator dose-response curves for four additional single active ingredients (in addition to those represented in Fig. 2A) identified from TCM library screen (6 nM to 400 μM) (2), measured by spectrophotometric enzyme activity assay and normalized to baseline activity. (n=3; bars represent propagated error).

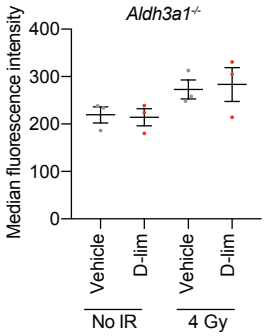

Fig. S4 DarkZone dye aldehyde levels in *Aldh3a1*$^{-/-}$ salisphere cells after 4 Gy or without radiation

Aldehyde levels in dissociated *Aldh3a1*$^{-/-}$ salispheres, 2 h after IR, treated with 100 μM D-limonene or vehicle control PEG-400, measured as median fluorescence intensity of DarkZone dye. (n=3; bars represent SEM; groups are not significantly different).

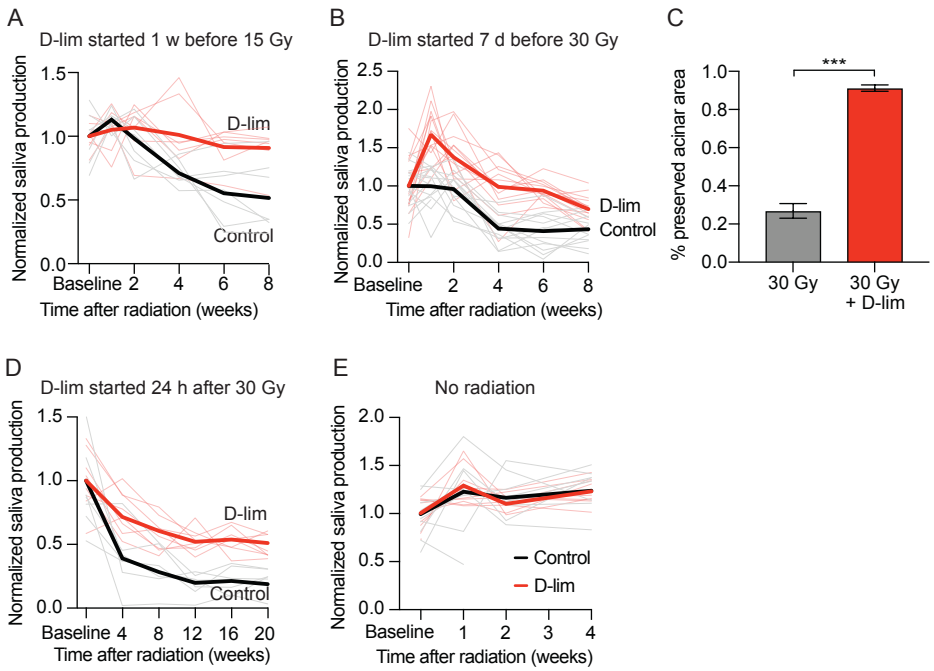

Fig. S5. Saliva production levels after IR in individual mice with or without D-limonene treatment

(A) Saliva was measured in female C57BL/6J WT mice at baseline and 1, 2, 4, 6, and 8 wk after a single dose of 15 Gy. Treatment group started 10% D-limonene in chow 7 d before IR, and control group received no treatment. (n=7-8; thick lines represent mean; thin lines represent individual mice; wk 1 p=0.4049; wk 2 p=0.3876; wk 4 p=0.0028; wk 6 p=0.0004; wk 8 p=0.0001). *(B)* Saliva was collected at baseline and at wk 1, 2, 4, 6, and 8 after 30 Gy (6 Gy/d). Treatment group received 10% D-limonene in chow starting 7 d before IR, and control group received no treatment. (n=12-15; thick lines represent mean values; thin lines represent individual mice; wk 1, 2, 4, 6 $p<0.0001$; wk 8 p=0.0087). *(C)* Quantification of SMG acinar area 8 wk after 30 Gy (6 Gy/d) by PAS staining (20x images), analyzed with ImageJ and normalized to nonirradiated glands. Treatment group received 10% D-limonene in chow starting 7 d before IR, and control group received no treatment (n=10; bars represent SEM, ***=$p<0.001$). *(D)* Saliva was measured in female C57BL/6J mice at baseline and every 4 wk after 30 Gy (6 Gy/d). Treatment group started 10% D-limonene in chow 24 h after final IR fraction, and control group received no treatment. (n=7-8; thick lines represent mean values; thin lines represent individual mice; wk 4 $p<0.0001$; wk 8 p=0.0016; wk 12 p=0.0001; wk 16 p=0.0003; wk 20 p=0.0059). *(E)* Saliva production levels in nonirradiated mice. Treatment group received 10% D-limonene in chow, and control group received no treatment. Saliva was measured at baseline and after treatment at wk 1, 2, and 4. (n=10 mice/group; thick lines represent mean values; thin lines represent individual mice; groups are not significantly different).

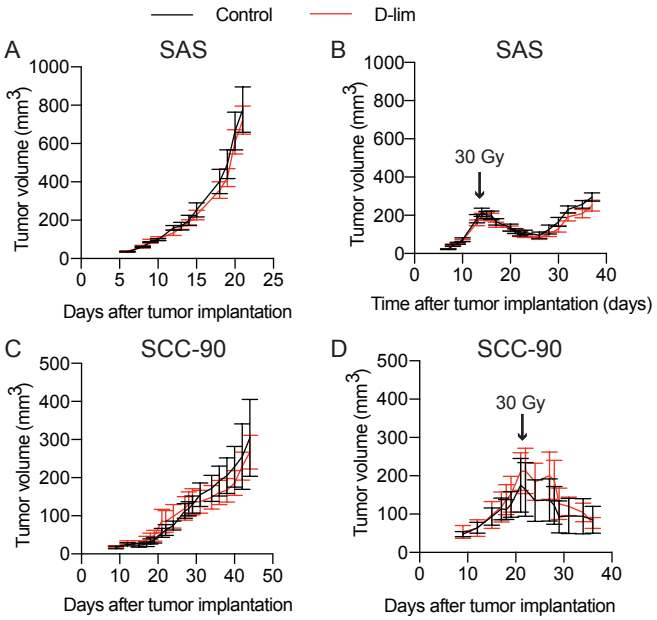

Fig. S6. Xenograft study in mice treated with or without D-limonene

(A) Tumor volume measured over time in nonirradiated SCID mice implanted with SAS cells. *(B)* Tumor volume measured over time in SCID mice implanted with SAS cells and irradiated with 30 Gy. *(C)* Tumor volume measured over time in nonirradiated SCID mice implanted with SCC-90 cells. *(D)* Tumor volume measured over time in SCID mice implanted with SCC-90 cells and irradiated with 30 Gy. All treatment groups received D-limonene in chow starting 7 d before IR, and all control groups received no treatment. (n=5; no significant difference between groups).

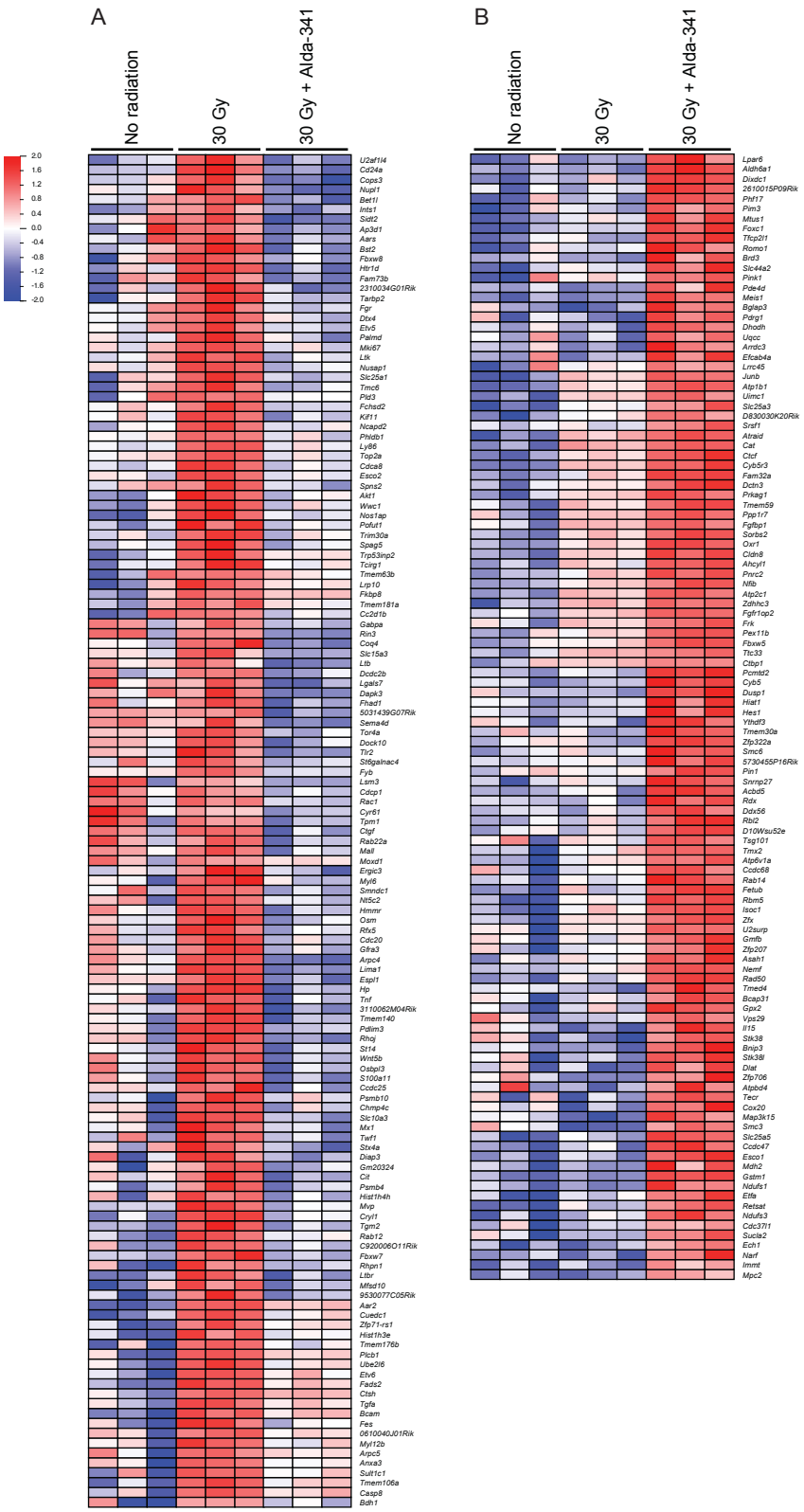

Fig. S7. Heatmaps of RNA-seq analysis

(A) Heatmap comparing RNA levels of immune-response related genes of EpCAM^{+} cells isolated from SMG of mice 2 wk after 30 Gy (6 Gy/d) or no IR. Treatment group received 10%

D-limonene in chow for 1 wk before IR and daily thereafter, and control groups received no treatment. (n=3 mice/group; 3 RNA samples/mouse). *(B)* Heatmap comparing RNA levels of genes related to glutathione metabolism.

A

Sample	Run 1 (ng/g)	Run 2 (ng/g)		
	Sample 1	Sample 2	Sample 3	Sample 4
Patient 1	7935	675.3	920.8	1546.5
Patient 2	1328	1156.4	1004.2	796.3
Patient 3	454	97	79.4	72
Patient 4		7284.7	3466	3481
Control 1		1.5	BQL	
Control 2		0	BQL	
Control 3		6.2	BQL	

B

Sample	Run 1 (ng/mL)	Run 2 (ng/mL)
Patient 1 (before)	4	1.7 (BQL)
Patient 2 (before)	6	0 (BQL)
Patient 3 (before)	8	0 (BQL)
Patient 1 (after)	149.1	145.4
Patient 2 (after)	243.1	235.5
Patient 3 (after)	39.9	27.9

C

Sample	Run 1 (ng/mL)	Run 2 (ng/mL)
Patient 1 (before)	0 (BQL)	
Patient 2 (before)	0 (BQL)	
Patient 3 (before)	0 (BQL)	
Patient 4 (before)		0 (BQL)
Patient 1 (after)	0 (BQL)	
Patient 2 (after)	9.5	
Patient 3 (after)	8.8	
Patient 4 (after)		11.7

Table S1. Phase 0 human study of D-limonene drug distribution in 4 patients

(A) D-limonene levels in human salivary gland tissue collected after 2 wk of 2 g/d oral D-limonene measured by GC-MS. *(B)* D-limonene levels in human plasma at baseline and after 2 wk of D-limonene treatment. Two samples per time point were analyzed. The 4th patient was unable to provide plasma, therefore only data for 3 patients are reported. *(C)* D-limonene levels in human saliva at baseline and after 2 wk of D-limonene treatment. One sample per time point was analyzed. BQL=below quantifiable limits.

References

1. Szlávik V, et al. (2008) Differentiation of primary human submandibular gland cells cultured on basement membrane extract. *Tissue Eng Part A* 14(11):1915-1926.
2. Chen C, Cruz L, Mochly-Rosen D (2015) Pharmacological recruitment of aldehyde dehydrogenase 3A1 (ALDH3A1) to assist ALDH2 in acetaldehyde and ethanol metabolism in vivo. *Proc Natl Acad Sci USA* 112:3074-3079.
3. Yuen L, Saxena N, Park H, Weinberg K, Kool E (2016) Dark hydrazone fluorescence labeling agents enable imaging of cellular aldehydic load. *ACS Chem Biol* 11:2312-2319.
4. Steinberg Z, et al. (2005) FGFR2b signaling regulates ex vivo submandibular gland epithelial cell proliferation and branching morphogenesis. *Development* 132:1223-1234.
5. Chen C, et al. (2008) Activation of aldehyde dehydrogenase-2 reduces ischemic damage to the heart. *Science* 321:1493-1495.
6. Schrödinger Release 2017-4: Schrödinger Suite 2017-4 Protein Preparation Wizard; Epik, Schrödinger, LLC, New York, NY, 2016; Impact, Schrödinger, LLC, New York, NY, 2016; Prime, Schrödinger, LLC, New York, NY, 2017.
7. Schrödinger Release 2017-4: Glide, Schrödinger, LLC, New York, NY, 2017.
8. Schrödinger Release 2017-4: SiteMap, Schrödinger, LLC, New York, NY, 2017.
9. Schrödinger Release 2017-4: LigPrep, Schrödinger, LLC, New York, NY, 2017.
10. Lombaert I, et al. (2008) Rescue of salivary gland function after stem cell transplantation in irradiated glands. *PloS One* 3:e2063.
11. Graves E, Quon A, Loo B, Jr. (2007) RT_Image: an open-source tool for investigating PET in radiation oncology. *Technol Cancer Res Treat* 6:111-121.